

Evolution of Gaits in a Simulated Hybrid Leg-Wheel Robot

Evolution von Gangarten eines Simulierten Hybriden
Bein-Rad-Roboters

Bachelor Thesis

University of Applied Sciences Bremen

International Studies of Biomimetics (B.Sc)

Kai von Szadkowski

Matriculation Number 227788

December 17, 2010

1st Advisor:

Prof. Dr. Susanna LABISCH
University of Applied Sciences,
Bremen

2nd Advisor:

Prof. Dr. Frank KIRCHNER
DFKI Robotics Innovation Center,
Bremen

Supervisor:

Jakob Schwendner, M.Sc.
DFKI Robotics Innovation Center, Bremen



ACKNOWLEDGEMENTS

First of all I would like to thank my two advisors, Prof. Dr. Susanna Labisch and Prof. Dr. Frank Kirchner, who both provided me with helpful insights along the way and without whom, of course, this work would not have been possible.

I also want to thank Jakob Schwendner, my supervisor at the DFKI, who had great confidence in this thesis from the start and encouraged me to take it on in the first place. Many thanks also go to Michael Rohn for his help with the installation of the MARS simulation and especially Malte Römmermann, who was always happy to provide advice on the intricate details involved in developing and tuning a plugin for an only marginally documented simulation environment, and additionally granted me access to the superior computation power of his computer.

I am also indebted to the other members of the Intelligent Mobility Project for the countless discussions about similarly countless elements of this work and their support and interest (as well as patience) throughout my thesis. This is especially true for Ajish Babu and a number of memorable and valuable conversations we had as well as Felix Grimminger, from whom I received helpful feedback on the realism of the simulated robot with respect to its real-life counterpart.

Finally, I would like to express my gratitude towards those other people who did go unmentioned here, but supported me nevertheless.

Contents

Acknowledgements	III
Abstract	1
1 Introduction	3
1.1 Mobile Robotics & Inspiration from Biology	3
1.2 Animal Motion Behaviour	6
1.2.1 Characterizing Gaits	6
1.2.2 Energy Efficiency & the Evolution of Gaits	8
1.3 Hybrid Robots: Wheels as Legs	9
1.3.1 Wheel Mechanics of Hybrid Systems	10
1.3.2 Specifics of the Modelled System: AsGuard	12
1.4 Evolutionary Computing	13
2 Materials & Methods	15
2.1 Simulation Environment & Plugins	15
2.1.1 The MARS Simulation	15
2.1.2 Design of Plugins	15
2.1.3 The Physical Robot Model	16
2.1.4 Tuning of the Simulation	17
2.1.5 Definition of the Robot's Gaits	18
2.1.6 Motor Controller	18
2.2 Evolution Experiments	20
2.2.1 Fitness Function	20
2.2.2 General Considerations & Approach	21
2.2.3 Validation of Methods & Initial Tests	21
2.2.4 Vertical Deviation of COM	23
2.2.5 Manually tuned Experiments	24

3	Results	25
3.1	Validation of Methods & Initial Tests	25
3.2	Vertical Displacement	26
3.2.1	Development of Fitness Values	26
3.2.2	Froude Numbers	26
3.2.3	Relative Phases & and Evolved Gaits	27
3.2.4	Ground Contact: Angles of Attack	31
4	Discussion	35
4.1	Validation of Methods & Initial Tests	35
4.2	Vertical Displacement	35
4.2.1	Development of Fitness Values	35
4.2.2	Froude Numbers	36
4.2.3	Gait Patterns	36
4.2.4	Angles of Attack	38
5	Conclusion	39
	Bibliography	41
	Declaration of Authorship	49

ABSTRACT / ZUSAMMENFASSUNG

Biomimetics offers great opportunities for the design of mobile robots, yet direct application of biological principles is problematic due to the complexity of biological systems. Hence hybrid systems incorporating elements both from biology and classical engineering are an increasingly popular branch of robotics. One such type of hybrid robots are systems using legged wheels as means of locomotion and are thus greatly restricted in their degrees of freedom and motion dynamics.

In this thesis, it is investigated in what aspects such reduced walking systems differ from their biological counterparts and to what degree they can still achieve diverse motion patterns as can be seen in the natural world, in particular distinct gaits. Apart from theoretical considerations, experiments were conducted with a physical simulation of a hybrid robot using an evolution strategy to evolve gait patterns.

The results suggest that it is at least under certain circumstances possible and sensible to treat hybrid walking robots as walkers rather than skid steers.

Bionik bietet großes Potential für das Design mobiler Roboter, jedoch ist eine direkte Übertragung biologischer Prinzipien aufgrund deren Komplexität problematisch. Daher finden hybride Systeme, die Vorteile aus Biologie und klassischem Maschinenbau vereinen, immer größerer Verbreitung. Ein Typ eines solchen Hybrids sind Systeme, welche beinbesetzte Räder zur Bewegung nutzen und daher nur eingeschränkte Freiheitsgrade und Dynamik besitzen.

In dieser Arbeit wurde untersucht, unter welchen Aspekten sich solche Systeme von ihren biologischen Vorbildern unterscheiden und wie sie dennoch verschiedene Gangarten nutzen können, wie sie in der Natur zu beobachten sind. Hierfür wurden neben theoretischen Betrachtungen Experimente mit einer physikalischen Simulation durchgeführt, wobei eine Evolutionsstrategie genutzt wurde, um Laufmuster zu entwickeln.

Aus den Ergebnissen lässt sich schließen, dass es unter bestimmten Voraussetzungen möglich und sinnvoll ist, hybride Laufroboter als richtige Läufer zu behandeln.

1 INTRODUCTION

1.1 MOBILE ROBOTICS & INSPIRATION FROM BIOLOGY

The natural world has always been an inspiration to the field of robotics, be it in providing examples for complicated mechanisms or sophisticated behavioural strategies (Thakoor, 2000; Noor et al., 2000; Ijspeert, 2008; Pfeifer et al., 2007; Scarfogliero et al., 2009). This is particularly true in the case of terrestrial mobile robotics, where aside classic engineering designs with wheels, a large number of robots utilising legs of some kind to provide means of locomotion have been constructed or envisioned (Todd, 1985; Quinn et al., 2001; Kirchner et al., 2002; Knight and Nehmzow, 2002), many of which used land-dwelling animals as templates.

Most of these robot walkers, however, present themselves to the present day as heavily simplified versions of their natural counterparts and commonly prove less robust and energy-efficient than wheeled systems (Kar et al., 2003; Ritzmann et al., 2004). There are good reasons for this, as animals are vastly complex systems, showing a number of elements still well beyond engineers' capabilities, such as many degrees of freedom (Ritzmann et al., 2004), microscopic material structures and regeneration (Chapman, 1998; Vincent and Wegst, 2004; Olszta et al., 2007) as well as sophisticated, distributed sensory and information processing systems (Nieuwenhuys et al., 1997; Chapman, 1998; Smith, 2009).

Nevertheless, many examples for dramatic advances in the field of biomimetic robotics can be found, such as McGeer's mechanical walkers in terms of efficiency (McGeer, 1990) or the application of CPGs for leg control (see Ijspeert 2008 for an overview). A lot of this progress can be attributed to the successful application of biological knowledge, be it descriptive methods or insights in fields such as biomechanics and neurophysiology, leading to an ever-growing ability to mimic nature. This has gone so far as to robotics giving back to biology by providing experimental settings to study different aspects of organisms in a simplified and modelled form (Webb, 1995).

As the complexity of bio-inspired robotic systems comes with certain previously mentioned drawbacks, it is not useful to blindly mimic nature when more robust and efficient solutions can be drawn from classic engineering. One way to address the particular dilemma of the robustness of wheeled systems and agility of legged systems is to create a hybrid between the two. The fundamental idea is to attach a leg to the body of a robot via one single rotary joint, shaped in such a way that a turning of it at this 'hip' joint will result in a motion resembling the movement of legs. There is more than one way to accomplish such a feat, the two most prominent possibilities being implementing a curved single leg or removing the rim of an ordinary wheel entirely, so that only the spokes remain. There are a number of robotic systems which follow this approach, such as Case Western's Whegs™ ([Allen et al., 2003](#); [Morrey et al., 2003](#); [Bachmann et al., 2009](#)), RHex ([Saranli et al., 2001](#); [Altendorfer et al., 2001](#)) originally developed at McGill University and the AsGuard ([Eich et al., 2008](#)), created at the German Research Center for Artificial Intelligence (DFKI) ¹ - all shown in Fig.1.1 . The advantage of these systems is their capability to traverse difficult terrain with the simplicity of actuating only one degree of freedom per leg, greatly reducing the complexity of control as well as mechanics and number of motors and sensors.

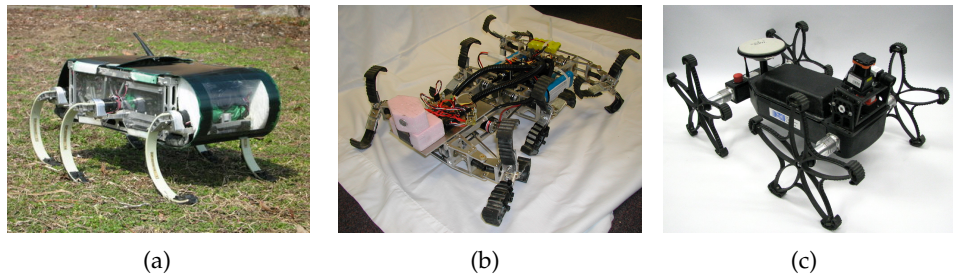


FIG. 1.1: The hybrid pseudo-walkers RHex (a), Whegs™(b) and AsGuard V3 (c)

As such hybrid systems are becoming increasingly popular among robot engineers, it seems to be a task worth undertaking to more closely examine properties of these 'pseudo-walkers' in order to develop ways to compensate for the inevitable loss of dynamics and thereby increase the variety of motion patterns of these systems, which has been undertaken for example on the RHex system ([McMordie and Buehler, 2001](#); [Weingarten et al., 2004](#); [Neville et al., 2006](#)) and also with AsGuard ([Babu et al., 2010](#); [Machowinski, 2009](#)). As stated in [Babu et al. 2010](#), such attempts have to struggle with the problem that "Analytical analysis possi-

¹German: Deutsches Forschungszentrum für Künstliche Intelligenz

bilities are limited due to several system complexities and non-linearities.” and proposes to conduct experiments to “[...] gain insight into the system properties.”.

In order to specify these properties, a reference frame providing adequate methods of description and comparison is needed, as the hybrid-nature of these systems poses the problem that they do not fit in one category or the other - they are neither true skid steers (i.e vehicles using differential drive), nor true walkers. However, the variation already evident in current pseudo-walker systems could be interpreted as a spectrum of locomotion between the two forms. So the question at hand is: where in this spectrum can a system like AsGuard be found?

To answer this question and thereby provide a basis for improving the motion patterns of pseudo-walkers, it seems like a promising approach to review the methods and parameters developed for analysis of biological walking systems and investigate to what degree they also apply to a simplified walker like AsGuard. This raises a number of further, yet less general questions, which this thesis seeks to investigate, such as:

- How useful are these methods from biology to characterise a hybrid walking system?
- Can such a system, just like animals, make use of different gaits?
- How can different gaits be realized in the first place given the few degrees of freedom?

This work seeks to answer these questions and is divided into three stages. First of all, the walking behaviours of animals and the methodology to describe and analyse them are reviewed. As a second step, a hybrid pseudo-walking robot for which the AsGuard serves as a blueprint is theoretically analysed along these lines. Finally, a large number of experiments were conducted with a physical model in a simulation environment, both manually tuned and with use of an evolutionary algorithm. The results of these experiments are then discussed with respect to the theoretical framework established before and finally conclusions are drawn addressing the initial questions.

1.2 ANIMAL MOTION BEHAVIOUR

Since early work of the 19th century (for example [Marey 1874; Muybridge 1887](#)), numerous studies have been conducted, yielding a variety of tools for the systematic and mechanical characterisation of terrestrial legged locomotion. For the sake of simplicity, in the following only quadruped animals will be considered.

1.2.1 Characterizing Gaits

When an animal moves, it shows a distinctive, repeated pattern of motions of its legs, called a *gait*. The minimal repeated gait elements are commonly referred to as a *stride*, or as [Alexander \(1984\)](#) phrased it: “a complete cycle of leg movements”, with one such leg movement called a *step*. In the majority of cases found in animals, each leg performs one step within one stride, either in parallel to the other legs or with a certain phase shift called *relative phase* or Φ . Normally one of the forefeet is chosen as the reference (receiving $\Phi = 0$) and the other legs’ relative phases are then defined as the fraction of the duration of a stride when the corresponding foot establishes ground contact. Practically all quadruped gaits can be classified with this scheme of strides and relative phases introduced by [McGhee \(1968\)](#) as illustrated in Fig. 1.2.

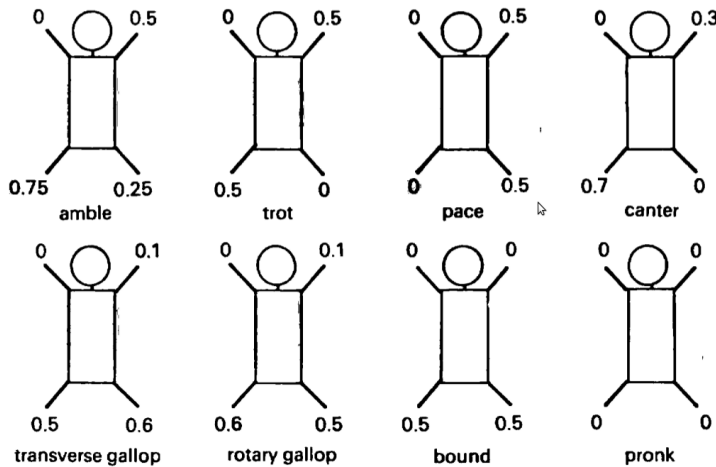


FIG. 1.2: Diagrams of a number of quadruped gaits with relative phases of leg movements and common names ([Alexander, 1984](#)).

McGhee further defined another variable called the *duty factor* (β) denoting the fraction of a stride during which a foot is in contact with the ground. Combining

this parameter with the ones mentioned before yields more differentiating diagrams of gaits, shown in Fig. 1.3. This enables for the useful distinction between symmetric and asymmetric gaits, the former describing such gaits where the left and right feet of the front and hind pair respectively show a relative phase shift of $\Phi = 0.5$ and equal values of β . Hence a horse's trot is symmetric whereas a gallop is asymmetric. This example also fits in the general pattern observed, namely that animals use symmetric gaits at lower speeds while using asymmetric gaits at higher speeds (Alexander, 1984).

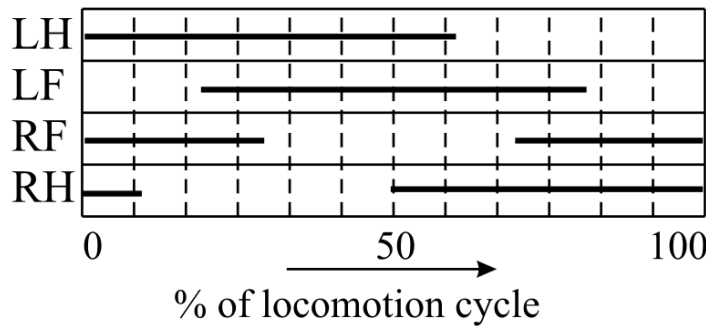


FIG. 1.3: A gait diagram with duty factors illustrated as length of the bars, taken from Kar et al. (2003).

Another common definition is that of 'walking' vs. 'running'. Gaits with $\beta > 0.5$ are considered walks, $\beta < 0.5$ denotes runs, the main difference being that walks show phases where both feet of an opposed pair are on the ground simultaneously. Alexander further defines the *stride frequency* f as the number of strides taken per unit time and the *stride length* λ as the distance travelled in a stride. Similarly the distance covered between two ground contacts of the same leg is called *step length* or κ .

Finally, the concept of *dynamic similarity* (Alexander and Jayes, 1983) has found useful application in gait analysis, as it enables the comparison of animals morphologically as diverse as for example mice and horses by finding constant scale factors between the specific dimensions, unit times and forces shaping their movement. One important aspect of dynamic similarity is that two systems move with the same Froude Number Fr, which is defined as

$$Fr = \frac{u^2}{g h} \quad (1.1)$$

where u is the speed of the animal, and h is a characteristic length, for which in

most cases the effective leg length (height of the hip joint over ground) is used ([Vaughan and O’Malley, 2005](#)). The Froude number allows to make predictions about the gait with which an animal travels at a given speed, as most quadrupeds perform gait transitions at the same values of Fr (see Fig. 1.4).

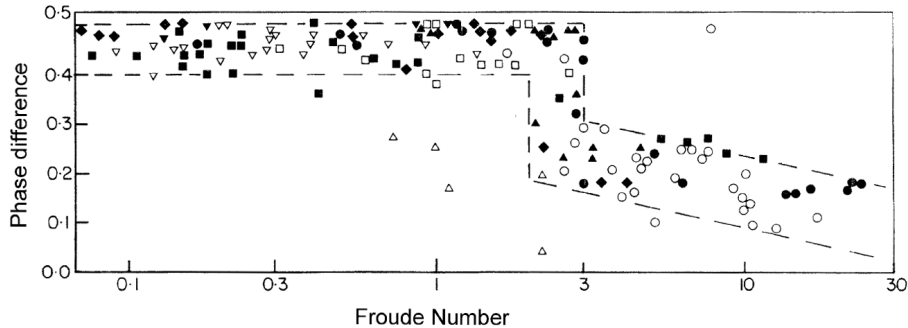


FIG. 1.4: Transitions from symmetrical to asymmetrical gaits of various quadrupeds such as dogs (●), ferrets (○) and rats (□) between $Fr=2$ and $Fr=3$, taken from [Alexander and Jayes \(1983\)](#).

These transitions have been found to occur at specific speeds, where one gait becomes more energy efficient than another ([Hoyt and Taylor, 1981](#)).

1.2.2 Energy Efficiency & the Evolution of Gaits

The gaits of animals have long been regarded as shaped by the interactions of evolutionary change and learning with energy efficiency as the foremost criterion ([Alexander, 1989](#); [Rayner, 2003](#)). Numerous studies have been conducted, yielding models to account for metabolism rates and muscle work (e.g. [Blanco and Gambini 2006](#)), spring-mass models (for instance [Blickhan 1989](#); [McMahon and Cheng 1990](#)) and models focusing on collisions (see for example [Ruina et al. 2005](#); [Bertram and Gutmann 2009](#)) and the resulting energy dissipation. For the purposes of this work, a collision-based model is particularly useful as it does not heavily depend on elastic properties, the influence of which is complicated in a system similar to AsGuard ([Babu et al., 2010](#)).

The central hypothesis of the aforementioned collisional model is that the energy expenditure during legged locomotion is mainly due to losses occurring when the center of mass (COM) of an animal (or robot) is redirected from a downward-moving direction to an upward-moving direction in the event of a collision between foot and ground, i.e. a step. The analogy used is that of a point

mass bouncing off the ground via a rigid strut representing a massless leg, thereby dissipating kinetic energy as a quadratic function of the *deflection angle* of the COM(Bertram and Gutmann, 2009). This angle equals the *angle of attack* α of the strut relative to the vertical to the ground. Hence many animals show gaits which especially at higher speeds seem to be 'designed' to avoid losses during collisions by reducing the angle of attack (Ruina et al., 2005). This of course only applies to animals that do not make extensive use of energy storage and recovery via elastic components such as tendons, the epitome of which may be found in kangaroos (Blanco and Gambini, 2006)

Note that related principles have also been considered before for the AsGuard robot by Babu et al. (2010), who argued that non-synchronised motion of the wheels leads to a reduction of vibrations and smoothing of the robot's movement by exchange of kinetic energy between different body parts.

The overall conclusions which can be drawn from these considerations are that a reduction of the vertical movement of the COM of the modelled robot as well as smaller contact angles of its legs upon ground contact could lead to a reduction of energy dissipation and smoother motion patterns.

1.3 HYBRID ROBOTS: WHEELS AS LEGS

There are two main components by which to discriminate between various hybrid systems, namely the number of the legs incorporated in a "wheel" and their shape, both of which are closely tied together. In fact, they act as constraints on one another since it is only possible to combine a certain number of legs of a certain spacial extent into a wheel. Consequently, different hybrid systems show different design approaches. RHex for instance uses legs bend into a long semi-circle forming rather large 'feet', hence only having one foot per joint, as can be seen in Fig. 1.1a. AsGuard on the other end of the spectrum incorporates five straight legs in one wheel (refer to Fig. 1.6(b) in the next section). In between and beyond that, examples can be found from the Whegs™family (Fig. 1.1b), which use various numbers and shapes of legs. But how exactly do these different designs influence the motion patterns and locomotive capabilities and characteristics of these robots?

1.3.1 Wheel Mechanics of Hybrid Systems

First the case of a rimless wheel having straight, rigid legs with equal angular difference (such a structure will be called a *star wheel*) traversing a flat horizontal surface will be considered. One single leg attached to the middle joint has no restraints on its motion. Depending on the state of the other legs of the robot, it is able to apply force to the ground with any angle of attack α between 0° and 90° . Adding another leg does not alter this, yet the step frequency doubles for constant angular velocities. The situation however changes dramatically when a third leg is introduced, as now exists a *double stance phase*, i.e. a phase in each step during which two of the legs are in contact with the substrate (Fig. 1.5).

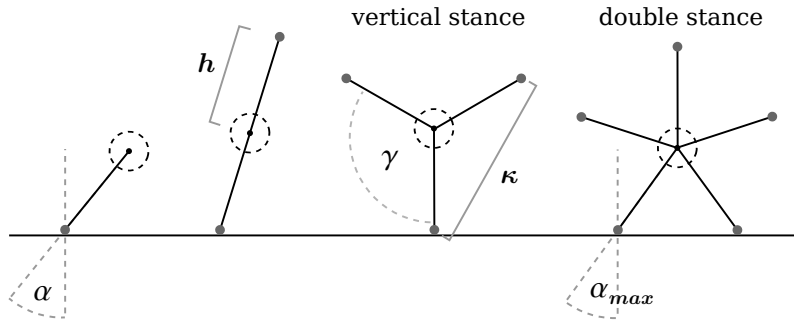


FIG. 1.5: Stance phases and parameters of star wheels. α : angle of attack, h : leg length, γ : angle between legs, κ : distance between feet (step length), α_{max} : maximum α .

The opposite of this case is the *vertical stance phase*, when only one leg is supporting the wheel as also shown in Fig. 1.5. Either way, a robot like AsGuard with four such star wheels (or wheels with more legs) is always in static equilibrium when standing or in approximation when walking slowly, independent of the wheels' orientation, which is an important difference to quadruped animals.

For obvious reasons, the maximum angle of attack is limited by the presence of two or more other legs and cannot become greater than in the double stance phase: it either decreases or another leg provides the supporting point. Hence α_{max} is determined by the angle between neighbouring legs and so, ultimately, by the number of legs n_l distributed over the circumference of the wheel:

$$\alpha_{max}(n_l) = \frac{\gamma}{2} = \frac{360^\circ}{2n_l} \quad \Rightarrow \quad 0^\circ \leq \alpha \leq \frac{360^\circ}{2n_l} \quad (1.2)$$

Tab. 1.1 contains the corresponding ranges of α for some values of n_l . But there is another consequence of n_l increasing. As the freedom of motion of each leg is reduced, so is the vertical motion of the wheel, i.e. the difference in height over ground Δz of the joint during vertical and double stance phase. This is an important characteristic parameter, as the robot has to overcome this height difference with every step (given that every foot establishes ground contact) so that the result is a vertical pendulum motion, leading to vibrations and energy dissipation, both in the motors and due to collision as outlined earlier. Given a leg length h and the maximum angle of attack α_{max} , it can be derived that

$$\begin{aligned}\Delta z &= h(1 - \cos \alpha_{max}) \\ \text{or, as a fraction of } h: \\ \Delta z_{frac} &= 1 - \cos \alpha_{max}\end{aligned}\tag{1.3}$$

for which a selection of values can also be obtained from Tab. 1.1. The implication of this is that the more legs per wheel a robot has, the closer the geometry of its hybrid wheels resemble an actual wheel (which is theoretically reached for $n_l \rightarrow \infty$), which always has an angle of attack of 0° and hence shows (in theory) no collisional energy dissipation. From this follows that more legs per wheel lead to a closer resemblance of the robots motion characteristics to those of a wheeled system and thus a better applicability of the approximation to treat it simply as a wheeled skid steer control-wise.

TAB. 1.1: Angle between legs γ and maximum angle of attack α_{max} for different values of n_l (number of legs) of a star wheel.

n_l	1	2	3	4	5	6	...	∞
γ	360°	180°	120°	90°	72°	60°	...	0°
α_{max}	90°	90°	60°	45°	36°	30°	...	0°
Δz_{frac}	1.0	1.0	0.5	0.29	0.19	0.13	...	0

The aforementioned statements are of course only true on a rigid surface, as any sinkage of feet or wheels in soft ground will change the angles in which force is exerted. The consequences are significant for star wheels: As the legs on one wheel are mechanically linked, subsequent ground contacts of any foot will be influenced by the previous foot of the same wheel. This makes a hybrid robot's behaviour hard to predict on such surfaces.

It seems, therefore, solely regarding energy efficiency and simplicity of control,

that there is no better option than the wheel. Leaving the somewhat theoretical case of a perfectly flat surface, however, this apparent advantage of wheels is relativised, as over rough terrain legged systems provide better traction and traversability ([Saranli and Buehler, 2000](#); [Kar et al., 2003](#)), and likewise hybrid wheels, for example by being able to climb obstacles as large as the distance of two neighbouring feet (see [Quinn et al. 2002](#) for an analysis of this issue).

This distance is equal to the step length κ during slow walking and indeed, as all wheels move simultaneously, to the stride length λ since the robot can not keep on moving with one wheel standing still, which is a constraint not present in animals. Hence, a hybrid pseudo-walker can only ever increase its stride length (and step length) by attaining a fly phase in its movement at higher speeds. From this directly follows that the duty factor in slow gaits necessarily has to be 1.0.

1.3.2 *Specifics of the Modelled System: AsGuard*

The actual AsGuard robot (Fig.1.6) has been reported on in other work ([Eich et al., 2008](#); [Babu et al., 2010](#)) and thus will not be discussed here in detail. However for the modelling of a similar system, one specific constructional detail is of interest: AsGuard does not simply consist of one rigid frame with four wheels but possesses a main body and a rear body connected by a passive, low friction rotary joint. This enables the system to maintain ground contact as it makes it harder for wheels to be lifted in the air especially on rough ground due to tilting of the robot's body. It also essentially rules out transmission of moments along the middle long axis from the front to the back and vice versa.

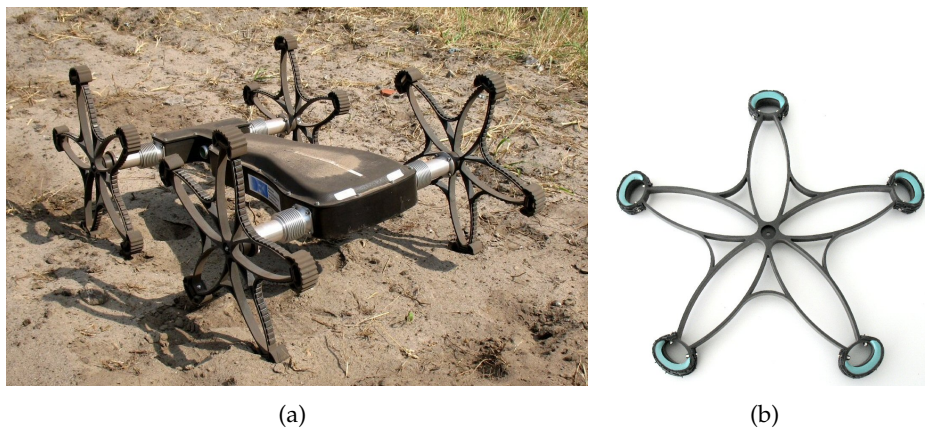


FIG. 1.6: The system used as a blueprint for the model in this work: AsGuard V2 (a) and a star wheel (b)

This additional degree of freedom could be regarded as an analogy to vertebrates, which also show degrees of freedom in their bodies' mid section due to flexibility of their spines (Gasc, 2001). However, this is less a rotary degree of freedom but rather a deformability in the sagittal plane (that is, the vertical plane along the long axis) which is also actively used for example in running motions (Alexander, 1989; Bertram and Gutmann, 2009).

1.4 EVOLUTIONARY COMPUTING

For development of optimised gaits, an Evolution Strategy (ES) was used in this work. Evolution Strategies are a family of numerical optimization methods which follow a stochastic approach inspired by biological evolution (Rechenberg, 2000; Hansen and Ostermeier, 2001). The definition of a solution to a given problem as a set of parameters allows for an implementation of an artificial evolutionary process by creating random configurations of such sets as *individuals* which are then mutated, recombined and evaluated for their fitness. This evaluation of course plays a vital role for success of the algorithm. Hence it is important that the so-called *fitness function*, which is mapping a parameter set \mathbb{R}^n to a *fitness value* $e \in \mathbb{R}$ (sought to be minimized in the process), constitutes an efficient way of judging a specific possible solution with respect to the specified goals.

The Covariance Matrix Adaptation Evolution Strategy (CMA-ES) is a sophisticated and fast algorithm originally developed at the Institute of Biomimetics and Evolution Technology at the TU Berlin (Ostermeier et al., 1994; Hansen and Ostermeier, 2001) and constantly improved (Hansen et al., 2003; Auger and Hansen, 2005) since. It is currently one of the most efficient evolution strategies for a wide variety of problems (Kern et al., 2004) and has previously been used for similar optimization of robot motion patterns (Römmermann et al., 2008), which is why it was also used in this work.²

²The latest version of CMA-ES implemented in C was obtained from Nikolaus Hansen's web pages on the website of the Laboratoire de Recherche en Informatique (LR) der Université Paris-Sud: http://www.lri.fr/~hansen/cmaes_inmatlab.html

2 MATERIALS & METHODS

2.1 SIMULATION ENVIRONMENT & PLUGINS

2.1.1 *The MARS Simulation*

All simulation experiments conducted during this thesis used the MARS¹ simulation environment which is being developed at the DFKI and is frequently used for a multitude of simulation tasks in research projects (see for example Römmermann et al. 2008).

MARS uses the Open Dynamics Engine (ODE) for three dimensional simulation of rigid body physics, which has been used in scientific work before (as for example Murphy et al. 2008). Graphical visualisation of the robot model is provided by MARS in real-time via the OpenSceneGraph library (Kuehne and Martz, 2007), enabling the user to study the motion behaviour of the simulated robot directly. This is an important part of the software, as it makes it possible to judge whether the robot shows a natural motion behaviour or if any of the movements seem implausible.

2.1.2 *Design of Plugins*

MARS allows to include external programs as plugins, providing an interface for control of the simulation and reading of simulation data. Two such plugins were developed for this work. The first combines the three major elements simulation environment, robot controller and evolutionary algorithm including fitness functions - the 'evolution plugin'. It also provides methods for data sampling during tests and data output of the simulation results. However, most of this data is dismissed during a running evolution after the test run of each individual as one set of evolutions can easily span over 50000 individuals and thus produces a massive excess of data. To still provide means of more detailed analysis on selected individuals produced by the ES, a second plugin ('batch-processing plugin') was

¹Machinae Arte Robotum Simulans

designed to read in a list of robot behaviours and log all the relevant data. This also allowed for fast experimenting with sets of pre-defined behaviours.

2.1.3 *The Physical Robot Model*

The physical model of the robot (see Fig. 2.1) used in this work was based on a model previously developed within the Intelligent Mobility project currently running at the DFKI and resembles the AsGuard V2 robot. It consists of a set of rigid bodies, namely the main body, the rear body and the four star wheels. A passive low friction joint with one rotary degree of freedom along its long axis connects the two body parts so that they can essentially turn freely with respect to each other. Major changes on the original model included improvement of geometric accuracy, refining the masses of the robot's body parts (now summing up to 9,6 kg) to establish the same COM position as in the real AsGuard V2 and correction of the friction in the body joint.

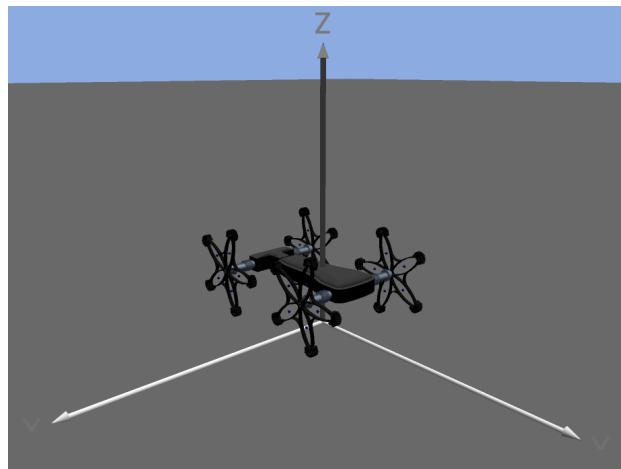


FIG. 2.1: The physical model of the robot in MARS.

Note that this model does not include any elastic elements such as springs, which is a major simplification, yet enables for fast computation, which was regarded an acceptable compromise. Another simplification concerns the motors used to drive the four star wheels. Rather than a complex motor model, simple motor controllers provided by ODE were used, which work as follows: a desired motor turning speed can be assigned to a motor which will then accelerate the joint to this speed within the next simulation iteration (time step). Friction effects in the joints or motors are completely ignored by this model. While this is of course

far from being realistic, it provides a simple way to accurately drive the wheels according to the controller. From this results that the controller parameters reflect the motion directly, so that their change over the course of an evolution can be directly interpreted.

For sake of simplicity the term 'robot' will in the following refer to the simulation model used in this work. In case an actual real robot is mentioned, this will be explicitly noted.

The robot's feet are represented by spheres and the plane on which the simulated robot walks is a completely horizontal and flat surface. It is not rigidly solid, however, but shows a small degree of 'softness'. This softness is not accurately defined in physical terms but rather by a set of parameters governing the error correction which handles the intersection of the simulated rigid bodies during iteration steps, allowing for objects to show a variety of collision behaviours, from fully elastic to somewhat energy-dissipating bounces.

2.1.4 *Tuning of the Simulation*

Two main criteria were used to determine the parameters for collision and friction between the robot's feet and the ground. First, visual inspection ruled out non-realistic behaviours which could neither be expected nor observed on the real-life counterpart of the robot. Second, readings of the torques applied by the motors were screened for different parameter sets. Finally, the values were tuned in on a configuration which allowed for nearly fragment-free graphs of these measurements as well as an overall naturally-looking behaviour of the robot (however, torque measurements were not used later, as the short contacts at higher speeds still created fragments). The Coulomb friction coefficient μ between ground and feet was set to 0.3, which is a rather low value but still valid for slightly slippery surfaces such as loose sand. However it has to be stressed that ODE uses a simplified version of Coulomb friction: instead of a friction cone which the theory proposes, a friction pyramid is used, rendering direct interpretations of μ difficult.

In conclusion, it has to be emphasized that the final configuration does not represent accurate physical values measurable in the real world, but rather a balanced system of model parameters resulting in an overall natural behaviour of the robot. In order to attain a more profound level of realism, extensive measurements of the real AsGuard V2 would have to be conducted to then tune the simulation to be

able to reproduce the exact results of them. As AsGuard was in this work merely used as a blueprint, this however was not necessary.

2.1.5 *Definition of the Robot's Gaits*

The definitions of animal gaits consist of two main components: footfall patterns and duty factors. Hence in order to model and evolve such patterns in a walking robot, a set of parameters has to be derived which account for both these elements. A few simplifying assumptions are worth making here. First of all, it is reasonable to exclusively regard gaits in which each foot only has one ground contact within one stride. By further assuming that every leg has the same phase duration of one stride, this allows to define a footfall sequence for a quadruped by defining one leg as a phase reference and defining three values of relative phases Φ of the other three legs in respect to the first one. In this work, the left forefoot (FL) was chosen as the static reference, with Φ_{FR} , Φ_{HL} and Φ_{HR} referring to the relative phases of the front right, hind left and hind right feet (wheels) respectively.

The case is more complex with duty factors, which are theoretically fixed at 1.0 at low velocities, but can be reduced by dynamic motions such as bounce or fly phases. Thus the duty factor is prone to variation, but cannot be directly specified; instead, it results from the defined relative phases and the way the legs move. Consequently, the leg movement will have to be specified by additional parameters specifying these motions to obtain a complete parameter set defining a gait, as will be laid out in the following section.

2.1.6 *Motor Controller*

A virtual motor controller was created to drive the motors and hence move the legs of the simulated model. One assumption which was followed when designing this controller was that the non-continuous geometry of the robot's wheels demands for a non-continuous driving model for the motors to make use of the wheels' geometry, so that different rotational speeds could be achieved during different phases of leg movement. The controller should both allow for a broad variety of different movements while at the same time use a reasonably small number of parameters to define these movements. However there is a limit to this trade-off as a vastly complicated motor driving function can be considered unrealistic and therefore seems rather not worth exploring in simulation in the first place. The final controller design reflects this trade-off and is depicted in Fig. 2.2.

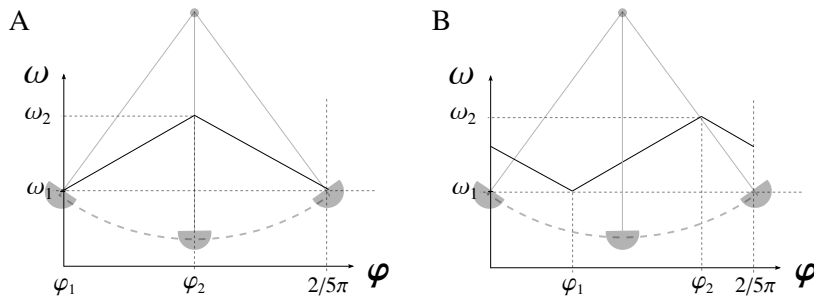


FIG. 2.2: Scheme of the controller used in the experiments. Over one fifth of a full rotation, i.e. γ , it defines the angular velocity ω as a function of the current angle φ as linear interpolations between two points specified by four parameters: $\omega_{1/2}$ and $\varphi_{1/2}$. This allows e.g. for a maximum of speed in the vertical stance phase (A) or high and low speeds at certain phases during a step (B).

It defines the angular velocity of the wheel ω as a function of its angular orientation φ using a set P of four parameters:

$$P = \{\omega_1, \omega_2, \varphi_1, \varphi_2 \in \mathbb{R}\}, \text{ with each of these parameters } p_i : 0 \leq p_i < 1 \quad (2.1)$$

with $\varphi_{1/2}$ representing two angles and $\omega_{1/2}$ likewise two corresponding angular velocities. As the wheel can be dissected into five equivalent parts, the controller function is only defined for a fifth of a full rotation, so that the values of $\varphi_{1/2}$ are mapped in a space of $0 \leq \varphi < \frac{2}{5}\pi$, with 0 describing the case where the current foot is the front leg of a double stance phase and $\frac{2}{5}\pi$ (or 1 in parameter frame) where it is the hind leg of a double stance position (which then is equivalent to the 0 position of the next leg). The four parameters are arranged in two pairs and thus specify two points in the possible value space, which are then linearly interpolated to determine values for the regions in between.

Given the three relative phases specified earlier, a robot gait can thus be defined as a set of seven parameters:

$$\mathcal{G} = \{\omega_1, \omega_2, \varphi_1, \varphi_2, \Phi_{FR}, \Phi_{HL}, \Phi_{HR} \in \mathbb{R}\} \text{ and again } 0 \leq g_i < 1 \quad (2.2)$$

The velocity parameters are not as restricted as the angles but must still be restricted to a pre-specified space in order to avoid nonsensical values produced by the evolutionary algorithm. Two mapping strategies are possible, namely $0 < \omega \leq \omega_{max}$ for forward driving and $-\omega_{max} \leq \omega < 0$ whereas the latter only

makes sense when the robot has to go backwards or is turning on the spot and therefore going backwards on one side in skid steer manner. In this work, only the first mapping was used.

This controller structure allows for a number of possible motions. The movement of the wheels can be accelerated and decelerated during one stance but also held constant if both values of ω are the same. By changing φ , the phase in which acceleration occurs can be altered so that maximum speeds can occur at any particular phase within one step. The controller therefore allows for a non-continuous driving of the wheels. Note however that it also has a number of restrictions. As it is based on angles and not time, the duration of a step will vary with the average speed resulting from the controller's function, therefore the step frequency cannot be directly specified. This means that in order for all four legs to have the same phase duration, they all have to use the same controller parameters (or at least a set of parameters resulting in the same average value of ω). Also, there is currently no limitation on the acceleration which can occur, so that unrealistic scenarios are possible if φ_1 and φ_2 differ only marginally while the corresponding values of ω_1 and ω_2 differ greatly. Furthermore it is not possible to specify the length of a phase of high or low speed - phases of high speed will always be shorter as those of low speed as the controller passes through the angular regions faster at higher speeds. This however is no drawback as it creates an impulsive motion of the leg resembling the steps of animals.

2.2 EVOLUTION EXPERIMENTS

2.2.1 *Fitness Function*

A variety of possible fitness parameters such as angles of attack or the robot's specific resistance calculated from the torque measurements were considered in preliminary tests for evaluation of the robot's performance. However most of the resulting fitness functions turned out impracticable due to simplifications in the model or rather inconclusive (some of the reasons for this will become apparent later). Finally, the deviation of the robot's centre of mass was chosen as the main fitness criterion for the evolutions analysed in this work, as well as its speed for validation of the simulation setup.

2.2.2 General Considerations & Approach

A time frame of 10000 ms was chosen for all experiments as a compromise between allowing sufficient movement also at low speeds and fast computation. The iteration or time step of the simulation was set to 10 ms (again a trade-off between speed and accuracy), thus 1000 iterations were calculated during one simulation run.

Setting the Relative Phases

As the motor controller maintains the offsets in phases between the wheels, it was sufficient to set the relative phase for each wheel once at the beginning of a test run. It is however not a good strategy to directly set the angles for the wheels offline. As they are oriented in double stance phase when the simulation is reset, any change in angle would result in collision errors and hence unrealistic behaviour upon start of a test run. Therefore the motor controllers were used to slowly drive the wheels into position while the simulation was running. This would sometimes result in slight turning of the robot, which was corrected if direction was crucial for the subsequent test. A driving strategy was developed calculating the turning speed for each time step with respect to the remaining distance between current (φ) and targeted (Φ) position as

$$\omega = 5 |\varphi - \Phi|. \quad (2.3)$$

This allowed for an accuracy of $10^{-4} rad$, which was set as the threshold for the difference under which the process would terminate.

2.2.3 Validation of Methods & Initial Tests

In order to validate the functionality of the developed software tools as well as the overall experimental approach a simple scenario was used: an optimisation for velocity. The fitness function for this case was defined as:

$$fit = \frac{1}{ds} \quad (2.4)$$

with ds being the distance the robot managed to move over the 10 seconds experimental time. For these experiments CMA-ES was set up with a dimension of $N = 7$, so that all seven gait parameters were subject to evolution. The maximum velocity for the motors was set to $\omega_{max} = 4\pi$ which equals two revolutions per

second.

This experiment was repeated several times over, in the course of which parameters of CMA-ES were tuned to fit the problem. A value of 0.5 for σ (the initial step size) was found to enable for reliable convergence (which lies in the vicinity of values recommended by the accompanying documentation). Also, the same termination criteria of the CMA-ES algorithm were determined and used in all evolutions following, namely a maximum for the number of generations G_n of $G_{max} = 500$ and a difference of the fitness values and movements in parameter space of less than $5 \cdot 10^{-3}$ between subsequent generations respectively.

As these three values are vital for the ES to successfully yield results and performance of the algorithm, they are worth being discussed more thoroughly. As for the maximum number of generations, it has to be noted that each evolution starts at a different essentially random position in parameter space. Given the step size, it thus takes a varying number of generations to arrive at a local or even global minimum of the fitness function. Obviously some initial positions are further away from such minima than others or less likely to reach due to properties of the algorithm. This effect can be quite dramatic, with some evolutions taking more than ten times the generations than others in the same setup to arrive at a comparable minimum (if they do at all). Hence, if the algorithm has not found a minimum after a considerable amount of time, it is reasonable to stop a particular evolution and invest the computation time in starting a new one. In most tests with varying setups, G_n would normally reach values of about 50-250, so that the chosen G_{max} was considered a reasonable upper margin.

Similar considerations apply to the minimum difference of fitness and parameter values. Changes of the evolved parameters of magnitudes lower than 10^{-3} do not significantly alter the robot's performance, so that any minor changes of such magnitudes can be safely dismissed as simulation fragments. Hence a lower value of this threshold would lead to the algorithm searching for an infinitesimally lower minimum of the fitness function on a nonsensical level, thereby wasting computation time. In some initial test cases with values of 10^{-4} and smaller, this was the case for large fractions of the total number of computed generations, so that finally a value was chosen that would in most cases still enable the evolution to find a minimum, but not scan around it excessively as a rather futile exercise.

2.2.4 Vertical Deviation of COM

As due to the many simplifications present in the model the energy expenditure derived from the torques of the motors did not prove reliable in preliminary tests, the vertical displacement of the COM was used as a proxy, following the argument presented in the introduction (section 1.2). Since this parameter is essentially dependent on geometrical constraints, it is more reliable than the modelled torques.

The fitness function for the experiments was defined as

$$fit = \sum_{i=1}^{n_i} |\bar{z} - z_i| \quad (2.5)$$

or, in other words, the cumulated absolute deviation from the average vertical position \bar{z} of the robot's COM.

Only the three relative phases Φ_{FL} , Φ_{HL} and Φ_{HR} were subject to evolutionary optimisation, while the other four parameters defining the motors' behaviour were set to two sets of fixed values (see Tab.2.1), denoting a mode of continuous driving (both ω_1 and ω_2 set to the maximum velocity, referred to as $mode_c$) and a mode of non-continuous driving ($mode_n$) with the highest speed at $\varphi = \frac{1}{5}\pi$, therefore resembling the example scheme from Fig. 2.2a.

TAB. 2.1: Fixed values of the four motor controller parameters during vertical displacement optimisation.

Parameter	$mode_c$	$mode_n$
ω_1	1.0	0.5
ω_2	1.0	1.0
φ_1	0.0	0.0
φ_2	0.5	0.5

Note that the two angles φ_1 and φ_2 of $mode_c$ do not influence the robot's behaviour as both ω values are 1.0.

Each experiment run included eight different values for ω_{max} in order to investigate possible optimal gaits at different velocities. In a first step, eight Froude numbers were specified, listed in Tab.2.2 (some of these might seem a bit odd, which is due to a calculation error that was corrected for afterwards). They were then transformed into rotational velocities of the wheels as follows: Equation 1.1 defining the Froude number can be rearranged to

$$u = \sqrt{\text{Fr} g h}. \quad (2.6)$$

Assuming that with every revolution of a star wheel five complete steps are taken, the distance covered per revolution is 5κ and thus, with the wheel turning at a frequency of ν , the robot's velocity equates to $u = 5\nu\kappa$, so that Eq. 2.6 can be transformed into

$$\nu = \frac{\sqrt{\text{Fr} g h}}{5\kappa} \quad (2.7)$$

and finally

$$\omega = 2\pi \frac{\sqrt{\text{Fr} g h}}{5\kappa}. \quad (2.8)$$

For the non-continuous mode, the thus obtained values were scaled by dividing them by the inverse of the average of ω ($\frac{1}{0.75} = 1.33$) in order to achieve similar Froude numbers as in the first run. All calculated values can also be viewed in Tab. 2.2.

TAB. 2.2: Froude numbers, turning frequencies and rotational velocities for the evolution runs optimising for vertical deviation

Fr	ν	$\omega_{max,c}$	$\omega_{max,n}$
0.08	0.346	2.175	2.900
0.24	0.600	3.767	5.023
0.40	0.774	4.863	6.484
0.56	0.916	5.754	7.672
0.80	1.095	6.878	9.170
1.20	1.341	8.423	11.231
1.60	1.548	9.727	12.969
2.00	1.731	10.875	14.499

For each of the resulting sixteen scenarios, 50 evolutions were completed.

2.2.5 Manually tuned Experiments

In order to allow for comparison with the results obtained from the evolution experiments, standard quadruped gaits depicted in Fig. 1.2 were manually implemented for the robot, both for continuous and non-continuous mode and various Froude numbers.

3 RESULTS

3.1 VALIDATION OF METHODS & INITIAL TESTS

A typical development of the fitness value over the course of the successive generations is depicted in Fig. 3.1. As can be clearly seen, the evolution rapidly develops towards a minimum of fitness values of about 0.045, which equals a travelled distance of approximately 22 m.

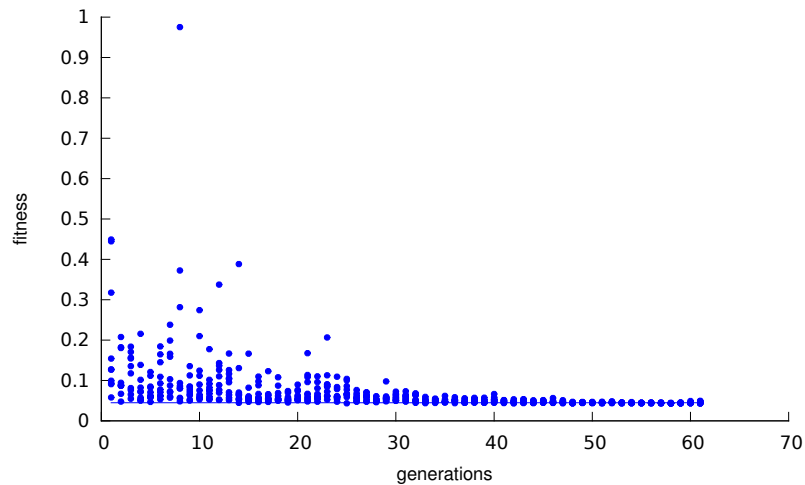


FIG. 3.1: Typical development of fitness function values over generations in the optimisation for speed ($N=7$).

In nearly all performed evolutions, both values for ω approached 1.0, while the other parameters showed no particular trend.

3.2 VERTICAL DISPLACEMENT

3.2.1 Development of Fitness Values

An example of the development of fitness values is shown in Fig. 3.2 for $\text{Fr}=0.56$ and mode_c . CMA-ES seems able to safely find parameter-sets approaching a minimum for the chosen fitness function, with improvement in comparison to initial values at a factor of 10 and larger. Similar developments can be observed for the other Froude numbers as well, although there is a trend towards larger fluctuations of the values at the time the algorithm stops for larger values of Fr.

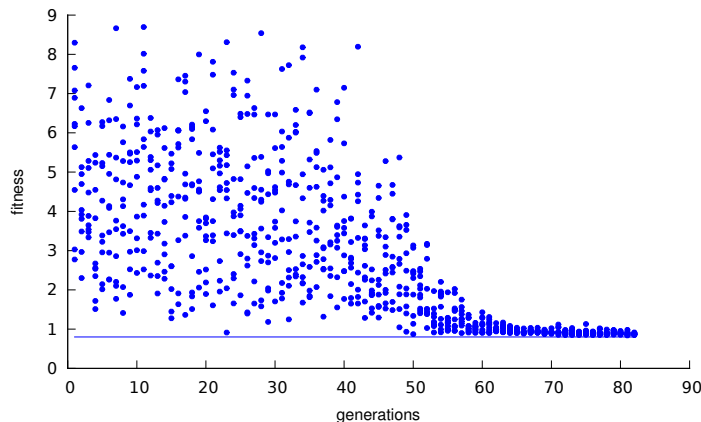


FIG. 3.2: Typical development of fitness function values over generations in the optimisation for vertical displacement with $\text{Fr}=0.56$ ($N=3$, mode_c).

The average fitness values reached by the evolutions are plotted in Fig. 3.3 and printed in Tab. 3.1. It becomes apparent that at lower Froude numbers the achieved fitness values are smaller and hence the achieved fitness higher than at larger Froude numbers. Also, the fitness values reached in non-continuous driving mode turn out lower than those in mode_c for $\text{Fr} \leq 0.8$ by initially 35 %. When comparing the best fitness (the lowest function values) to the averages of the 50 runs, the difference starts out small for both modes and reaches about 10 % for higher speeds.

3.2.2 Froude Numbers

The resulting Froude numbers calculated from the achieved speed ($\bar{\text{Fr}}_{\text{res}}$) are lower than the values initially targeted (Tab. 3.1). The deviation is larger for the non-continuous driving scenarios and increases as speed increases, reaching

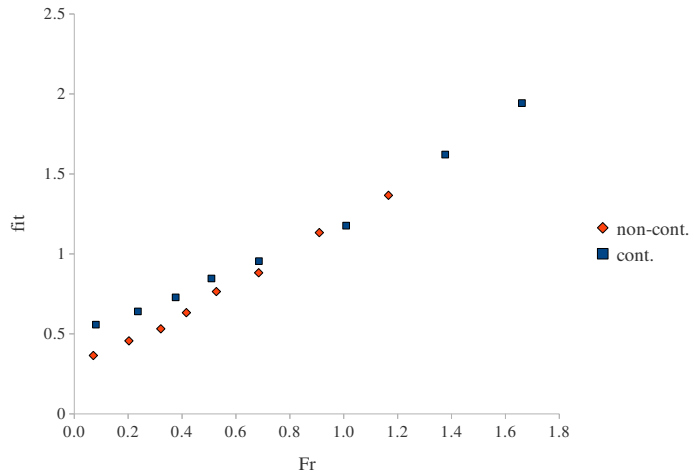


FIG. 3.3: Average fitness values achieved for each of the eight scenarios over average Froude number, both for continuous and non-continuous driving of the wheels.

41 % for the highest values of Fr in comparison to 17 % in the continuous case. This difference is larger though than the difference of the actual speeds as Fr is calculated from the square of u .

3.2.3 Relative Phases & and Evolved Gaits

Fig. 3.4 shows a collection of sets of Φ for some of the evolution scenarios, with the 50 evolutions of each are plotted with ascending values of Φ_{FR} . At low Froude numbers, three distinct gait patterns can be identified in both driving modes, an example given for $Fr=0.08$ and $mode_c$ in Fig. 3.4(a). These three gaits will be referred to as \mathcal{W}_1 , \mathcal{W}_2 and \mathcal{W}_3 respectively. Φ_{FR} obtains one of three values: 0.3 in \mathcal{W}_1 , 0.5 in \mathcal{W}_2 and 0.7 in \mathcal{W}_3 . Φ_{HL} and Φ_{HR} are then determined at values of approximately 0.55 and 0.75 (\mathcal{W}_1), 0.25 and 0.75 (\mathcal{W}_2) as well as 0.25 and 0.45 (\mathcal{W}_3) respectively.

These gaits are practically identical in the non-continuous case (a slight variation of \mathcal{W}_1 can be found with $\Phi_{FR} = 0.25$, which will be referred to as $\mathcal{W}_{1,0.5}$) and are maintained over rising speed up to $Fr=1.01$ (Fig. 3.4(b)) for continuous and $Fr=0.69$ for non-continuous driving (Fig. 3.4(e)) without significant changes. However at these Froude numbers, two of the three identifiable levels for Φ_{FR} have changed in $mode_c$, the lower moving to about 0.2 (which results in a modified gait which will be called \mathcal{W}'_1) and the larger to about 0.8 on average (they are also wider

TAB. 3.1: Combined results of both runs and all scenarios of the vertical displacement minimisation evolutions.

$\omega_{1/2}$	scen.	Fr_{set}	\bar{Fr}_{res}	$\bar{u}[m^{-1}]$	fit_{best}	\bar{fit}	s_{fit}
1/1	1	0.08	0.080	0.387	0.545	0.558	0.015
	2	0.24	0.236	0.663	0.623	0.640	0.021
	3	0.40	0.376	0.837	0.697	0.728	0.033
	4	0.56	0.509	0.974	0.803	0.846	0.050
	5	0.80	0.685	1.130	0.870	0.955	0.052
	6	1.20	1.009	1.371	1.064	1.177	0.048
	7	1.60	1.376	1.601	1.426	1.621	0.123
	8	2.00	1.661	1.759	1.809	1.943	0.076
0.5/1	1	0.08	0.071	0.363	0.357	0.365	0.010
	2	0.24	0.203	0.615	0.445	0.456	0.016
	3	0.40	0.321	0.773	0.507	0.532	0.048
	4	0.56	0.416	0.880	0.605	0.632	0.025
	5	0.80	0.527	0.991	0.709	0.764	0.056
	6	1.20	0.684	1.129	0.768	0.882	0.074
	7	1.60	0.909	1.302	1.035	1.133	0.086
	8	2.00	1.166	1.472	1.217	1.366	0.121

distributed), while \mathcal{W}_2 appears to be largely untouched. A wider distribution also holds true for the non-continuous case, where the three levels can now on average be identified at about 0.15, 0.45 and 0.8.

Further increasing speed, \mathcal{W}_3 transforms into a modified gait \mathcal{W}'_3 in continuous driving, with $\Phi_{FR} \approx 0.85$, as well as $\Phi_{HR} \approx 0.55$ and $\Phi_{HL} \approx 0.25$ (Fig. 3.4(c)), now not arbitrarily exchangeable any more. At the highest Froude number of 1.66 (Fig. 3.4(d)), distinct gaits disappear and instead, a continuum can be observed, showing values for Φ_{FR} of anything from 0.2 to 0.75 (with two single cases of 0.15 and 0.95).

The case is different for non-continuous driving of the wheels. Here \mathcal{W}_2 has disappeared at $Fr=0.91$ and again two distinct gaits are left: \mathcal{R}_1 (with $\Phi_{FR} \approx 0.1$ and Φ of the hind legs either 0.25 or 0.55) and \mathcal{R}_2 ($\Phi_{FR} \approx 0.9, \Phi_{Hx} \approx 0.4/0.15$) with again apparent arbitrary exchangeability of Φ_{HL} and Φ_{HR} . There is however the indication of a steep slope between these two by three intermediate results.

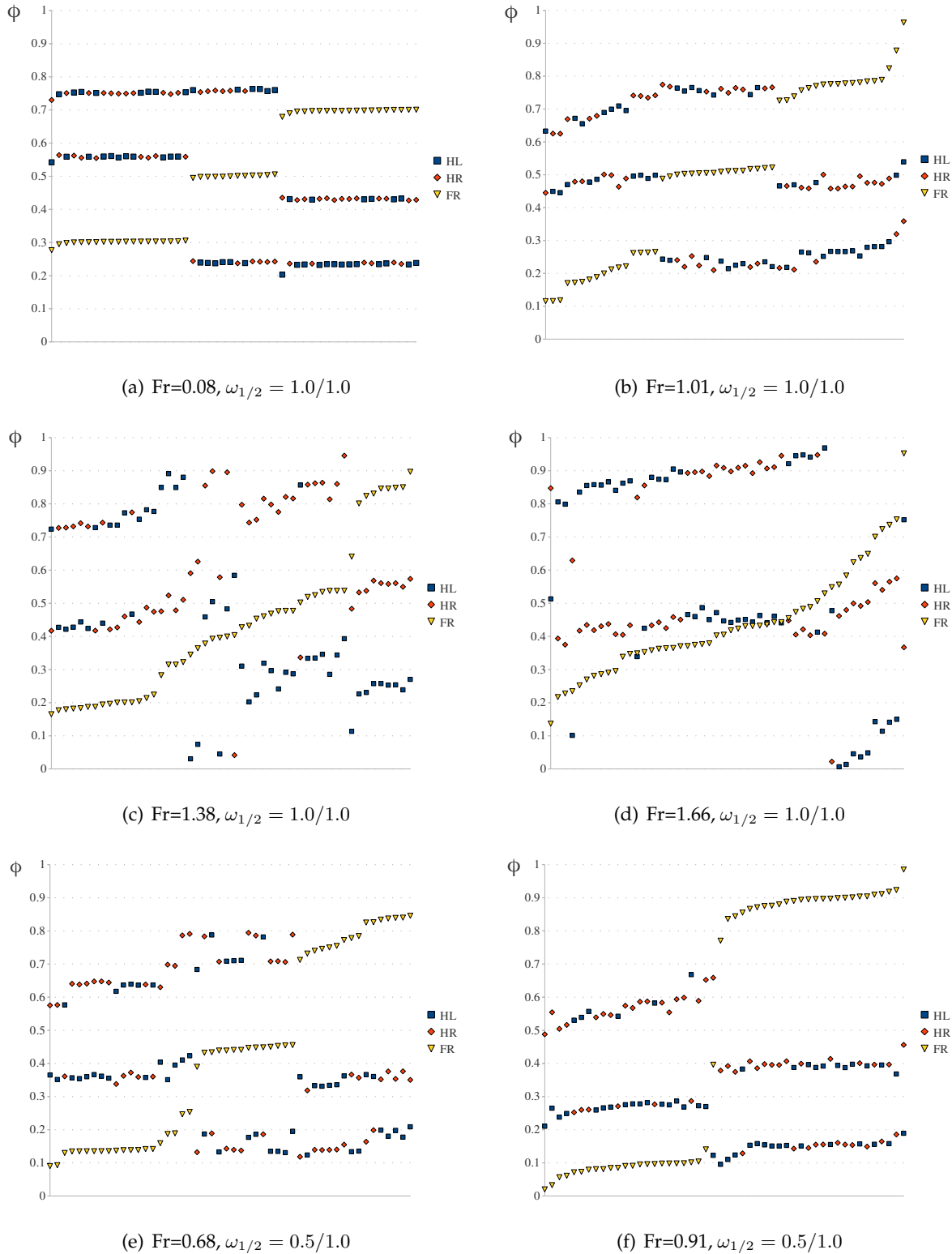


FIG. 3.4: Evolved relative phases for optimisation of vertical displacement for selected scenarios, ordered for ascending values of Φ_{FR} .

The evolved gaits are depicted in Fig. 3.5 and Fig. 3.6 (note that there are no gait diagrams for slow gaits as the duty factor is constantly 1 here).

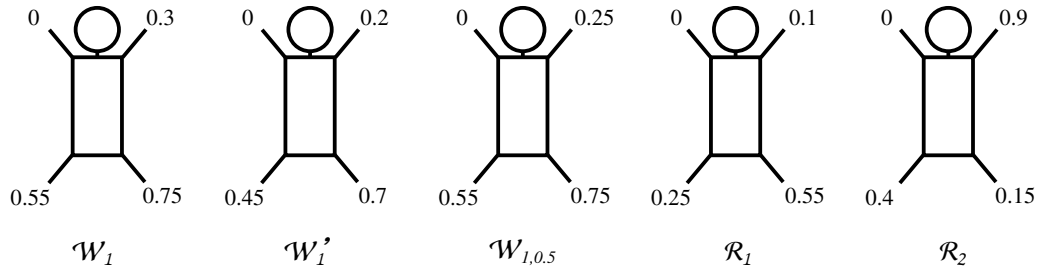


FIG. 3.5: Relative phases of selected evolved gaits (illustration inspired by [Alexander 1984](#)). Values of Φ_{HL} and Φ_{HR} are chosen arbitrarily where applicable.

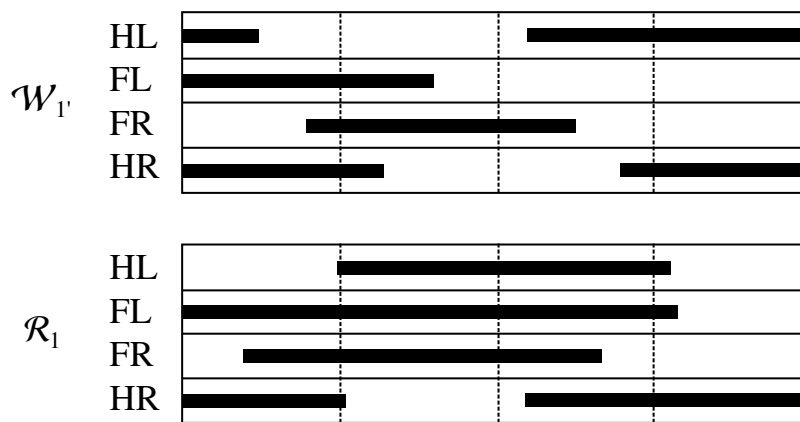


FIG. 3.6: Gait diagrams for two of the gaits observable at higher speeds.

Fig. 3.7 draws a comparison between evolved gaits and ‘classic’ gaits also used by [Babu et al. \(2010\)](#) by plotting the average vertical deviation of the average COM position (calculated from their fitness values) over a range of Froude numbers between 0 and 2.5. The classic gaits are a ‘pronk’¹, where all wheels are perfectly aligned, and a ‘trot’, where there is a half-phase offset between diagonally opposed wheels (refer to Fig. 1.2).

In continuous driving mode, the deviation values first slightly rise in the case of pronking, then decline from $Fr \approx 0.75$ and end with a high value of about 10 mm at $Fr \approx 0.4$. Trot and W'_1 perform more or less equally, with a minimum around $Fr \approx 1.3$ and rising again beyond that. W_1 on the other hand steadily increases over the whole range.

¹In fact, this gait is only a real pronking motion when there is a fly-phase between simultaneous ground contacts, but the term will be used for any fully aligned gait here.

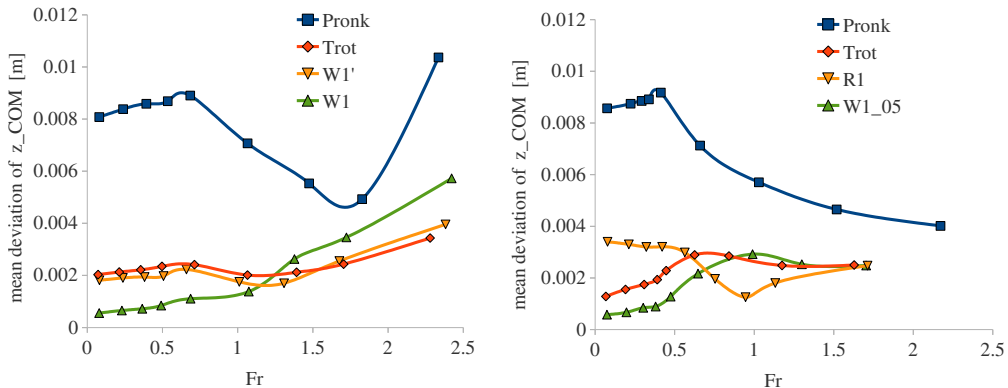


FIG. 3.7: Mean vertical deviation of the COM from its average vertical position for selected gaits over varying Froude numbers for both $mode_c$ (left) and $mode_n$ (right).

Non-continuous gaits show a different development over Fr. Pronking first develops similarly, but does not show an abrupt increase immediately after Fr=2.0. Trotting resembles $\mathcal{W}_{1/0.5}$ rather than a running gait, while \mathcal{R}_1 shows a distinct minimum at Fr=0.9 and then converges with the former two gaits at Fr=1.7.

A direct comparison is drawn in Fig. 3.8 between the performance of the evolved gaits and the two classic gaits pronking and trotting. While pronking, the COM shows vertical motions with amplitudes of ca. 15 mm at low speeds and ca. 10 mm when moving faster for both driving modes. The amplitudes are clearly reduced for the trot, ranging from approximately 3.5 mm in continuous mode to about 2.5 mm in non-continuous mode at low speeds and approximately twice these values at higher speeds. Finally the evolved gaits show the lowest amplitude, with less than 1.5 mm amplitude at low speed in continuous mode and even less in non-continuous mode. At higher velocities they show about the same amplitudes as the trot for continuous driving, and about half the amplitudes reached with trot when driving non-continuously.

3.2.4 Ground Contact: Angles of Attack

No correlation could be found between the magnitude of the vertical movements of the COM and the observed angles of attack. If anything, the evolved gaits seem to exhibit slightly larger values of α at given speeds than classic gaits, while there seems to be an overall strong negative correlation between travel velocity u and α as can be seen from Fig. 3.9.

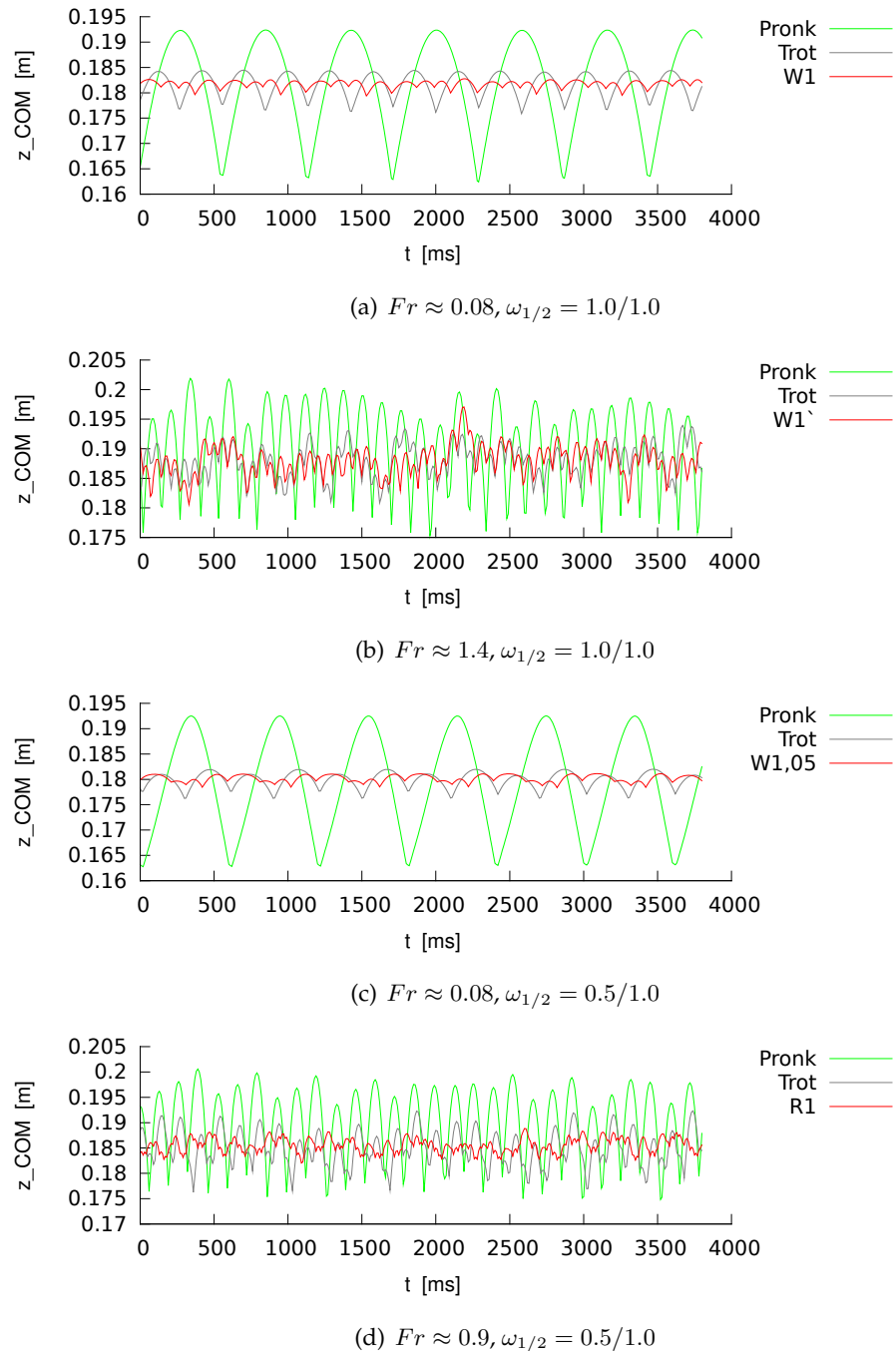


FIG. 3.8: Height over ground of COM over time for continuous (a, b) and non-continuous driving (c, d) with different gaits.

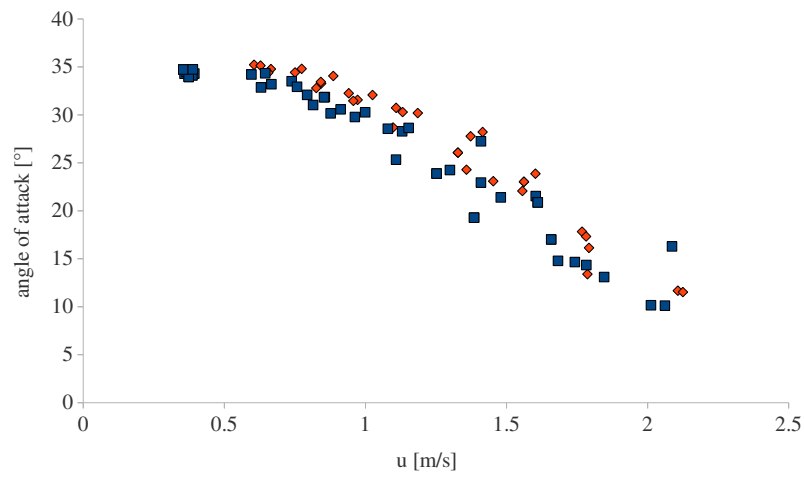


FIG. 3.9: Angles of attack (α) on the left front wheel over speed for all scenarios described in the previous section. Evolved gaits are plotted in red (\diamond), classic gaits in blue (\square).

4 DISCUSSION

4.1 VALIDATION OF METHODS & INITIAL TESTS

It becomes evident from the small number of generations needed to converge on a minimum of the fitness function that the application of the CMA-ES algorithm in the developed plugin as well as the tuning of its parameters were successful. However it has to be stressed that in this particular scenario, only two of the seven dimensions, namely ω_1 and ω_2 seemed to have had a considerable influence on the simulation outcome, so that this can essentially be regarded as a two-dimensional problem, hence the quick convergence. Consequently the relative phases seem to have no significant influence on speed. The fact that the two rotational speed parameters were maximized to 1.0 is not surprising, as this yielded the maximum speed possible within the given restrictions.

Overall, it can be stated that the simulation with the given settings can yield reasonable, predictable results and seems to work well combined with CMA-ES. To this could be added that visual inspection during the running experiment also showed that, judging from the motion of the wheels, the implementation of the motor controller seemed to work as intended.

4.2 VERTICAL DISPLACEMENT

4.2.1 *Development of Fitness Values*

The fluctuation of fitness values at higher Froude numbers and hence effectively higher speeds might be explained by the tendency of the robot to behave more chaotic when going faster. This would result in possibly larger influences of changes at the same scale of the evolving parameters compared to lower velocities and hence lead to the larger standard deviations of the fitness values. While higher precision in CMA-ES' termination criteria could perhaps reduce these fluctuations (although they were not altered when some evolutions were repeated with an

increase of precision by one order of magnitude), this would not solve the overall problem, namely that solutions are less robust at higher speeds.

For the same reasons, one might question the significance of the observed differences in minimum fitness evaluation values between continuous and non-continuous driving, especially at lower velocities. As more detailed analysis of the robot's performance showed clear differences between the two modes, it seems however unlikely that these differences are simulation fragments. A possible way of testing this could be to conduct evolutions with a wide range of values for ω_1 and try to identify trends of the best fitness values.

4.2.2 Froude Numbers

It is interesting that the velocities reached by the robot were lower than intended and the values reached in non-continuous driving constantly lower than the ones in continuous-mode, albeit the lower average wheel turning speeds were compensated for. A possible explanation for this is that the calculated friction forces between ground and the robot's feet were reduced due to bouncing motions. This would both account for the differences in velocities not only between driving modes, but also between different gaits within the same mode (although these were generally lower) and could further explain why the deviation increases over speed, as higher speeds result in more bouncing motions (expressed by reduced duty factors and larger vertical displacement of the COM). Another influence to explain the differences between the two modes is the difference in velocity with which the feet hit the ground, as it varies over φ and therefore α in the case of non-continuous driving as collisions do not occur at the same phase in all gaits.

4.2.3 Gait Patterns

The three distinctive parameter sets which were evolved for low Froude numbers can be classified as 'amble'-like gaits (see Fig. 1.2 or [Alexander 1984](#)). In fact, \mathcal{W}_2 is a textbook-amble with merely variation in the hind 'legs'. This is an interesting finding as ambles are classically used by quadrupeds at low velocities ([Alexander, 1989](#)). Another implication of this is that it seems to be conducive for a smooth walking motion to distribute the collisions over a stride as widely as possible.

A closer look at \mathcal{W}_1 and \mathcal{W}_3 reveals that they are mirror-images of each other. If FR is chosen as the first foot with ground contact in a stride, this shifts the values of Φ of the other legs by 0.3, so that FL follows with a relative phase of 0.3 and the

hind legs with 0.55 and 0.75 respectively, thereby matching perfectly with \mathcal{W}_1 . It is however unclear why these gaits deviate from a ‘perfect’ relative phase of 0.25 (as seen in \mathcal{W}_2), by a shift of about 0.05 in the second front and one hind leg, which is not random but appeared in many evolutions with almost no deviation. The reasons might be found in the specific geometrical and mechanical setup of the robot, the latter of which could also account for the interchangeability of the hind legs’ relative phases: as practically no moment is transmitted along the robot’s long axis due to the passive body joint, it might to some degree (and especially at low speeds where constant ground-contact virtually blocks a rotation around the vertical axis) be irrelevant which of the two hind legs induces a forward-movement at a given phase. Also, due to the same principles as explained above, \mathcal{R}_1 and \mathcal{R}_2 are also mirror images of one another, showing a resemblance to (transverse) galloping gaits.

Slight changes of gait parameters over speed without completely changing the overall motion pattern as found in the results can also be found in nature and can be regarded as a result from changing body dynamics ([Gasc, 2001](#)). Interestingly, the distinct gaits seen in lower speeds diffuse into a slope in continuous driving mode (with minor intermediate changes), but completely novel gaits appear in $mode_n$ at Froude numbers beyond 0.9. This can be regarded as evidence for the hypothesis that a non-continuous mode of driving the robot’s wheels enables it to more accurately emulate gait patterns as found in nature, yet it is still unclear what happens at higher speeds and Froude numbers. However the duty factors observed do not underline this, as for example \mathcal{R}_1 shows duty factors larger than 0.5 and hence can not be considered a running gait in the classic sense.

Another interesting fact is that the robot seems to switch from symmetric to asymmetric gaits at significantly lower Froude numbers than animals do ([Alexander, 1989](#)), where this transition occurs beyond $Fr=2$, and in $mode_n$ still earlier than in $mode_c$ (see Fig. 3.7). A reason for this might lie in the geometric differences between those two systems, which to some degree neglect the hypothesis of dynamic similarity between them, resulting in different transition Froude numbers. However, this might be corrected for by describing the robot’s motion more precisely: As there is no phase present in a gait where the robot has to swing its legs back to a frontal position, the step length of each leg is significantly reduced. If for example this missing phase takes about the same time as the duty phase, the ground covered for each step is doubled. Hence the step length of a hybrid robot is about half as long as an animal step length given identical leg lengths, so that

its equivalent leg length is $0.5 h$, resulting in doubled Froude numbers for given speeds. This would bring the observed transitions in ranges resembling those of quadrupeds.

Again, it would be necessary to conduct further evolutions with different values of ω_1 or even different leg lengths to clarify in how far the non-continuous driving influences the transition behaviour and in how far scaling methods with equivalent measures do generally apply.

Concerning the improvement which was accomplished by the evolution, it is obvious upon review of the vertical movement of the COM over time that the evolved gaits are far superior than fully-aligned driving (pronking). The improvement is less dramatic in comparison to a trot gait, but still significant especially in non-continuous driving. Nevertheless, these results suggest that there is a potential to reduce unwanted vibrations in the system via speed-specific gaits.

4.2.4 *Angles of Attack*

No connection could be found between values for α of the four feet and fitness values of the corresponding gaits. Instead, speed and therefore the rotation frequency of the wheels seems to largely influence the angles of attack, which casts doubt on the initial assumption that vertical movement is indeed related to energy efficiency in this system as fitness generally decreases with speed.

From Fig. 2.6, it can be seen that α hardly changes at for $u < 1\text{m}^{-1}$, which suggests that the overall movement is slow enough for gravity to constantly pull the robot on the ground. However at speeds of 2.0m^{-1} , bouncing motions or even fly phases of the robot (depending on the gait) allow for a significant reduction of α . This could explain why there is no direct connection to vertical displacement of the COM: as speed increases, the robot bounces more, but its wheels also move too fast to allow for it to “fall” down with each step, hence both phenomena effectively work against each other.

5 CONCLUSION

The results presented in this work do not paint a clear picture answering the initial question: Where can hybrid robots like AsGuard be found in the envisioned spectrum of locomotion? However a clear and simple answer could not have been expected, as the hybrid nature of such robots necessarily demands to show elements of both end stages. And this is exactly what the results suggest.

While different, defined gaits resembling those of natural systems emerge at different speeds and the system is thereby able to reduce bouncing motions, the angles of attack seem mainly independent of the gaits but rather scale with angular velocity of the wheels. Parallels show up between continuous and non-continuous driving modes for some speeds and parameters, while for other scenarios they differ greatly.

In spite of these ambiguous results, the results presented here suggest that the application of methods from biology to characterise hybrid pseudo-walking robots provides useful means to define different gait patterns for such robots and describe them with a set of parameters. It also became clear, however, that some of these parameters, such as the Froude number, will have to be redefined to enable for useful comparisons.

As for the applicability of these results, which were drawn from a heavily simplified model, on a real robot, further work is needed to account for the greater complexity of real systems, for example in terms of elastic components or motor controllers. Nevertheless, one study has previously shown results which may suggest that for example the distributed gait patterns which were evolved here could also lead to a smoother motion on a real robot ([Babu et al., 2010](#)). This vision becomes especially interesting with respect to current work on the real AsGuard robot, which aims to create an autonomous system, for which of course a better understanding of its motion dynamics could be highly valuable.

BIBLIOGRAPHY

Alexander, R. The gaits of bipedal and quadrupedal animals. *The International Journal of Robotics Research*, 3:49–59, 1984.

Alexander, R. M. Optimization of gaits in the locomotion of vertebrates. *Physiological Review*, 69:1199–1227, 1989.

Alexander, R. M. & Jayes, A. A dynamic similarity hypothesis for the gaits of quadrupedal mammals. *Journal of Zoology*, 201:135–152, 1983.

Allen, T., Quinn, R., Bachmann, R., & Ritzmann, R. Abstracted biological principles applied with reduced actuation improve mobility of legged vehicles. In *Proceedings. 2003 IEEE/RSJ International Conference on Intelligent Robots and Systems*, 2003.

Altendorfer, R., Moore, N., Komsuoglu, H., Buehler, M., Brown, H., McMordie, D., Saranli, U., Full, R., & Koditschek, D. Rhex: A biologically inspired hexapod runner. *Autonomous Robots*, 11:207–213, 2001.

Auger, A. & Hansen, N. A restart CMA evolution strategy with increasing population size. In McKay, B. et al., editors, *The 2005 IEEE International Congress on Evolutionary Computation (CEC'05)*, volume 2, pages 1769–1776, 2005.

Babu, A., Joyeux, S., Schwendner, J., & Grimminger, F. Effects of wheel synchronisation for the hybrid leg-wheel robot asguard. In *Proceedings of International Symposium on Artificial Intelligence, Robotics and Automation in Space (iSAIRAS-10)*, 2010.

Bachmann, R. J., Boria, F. J., Vaidyanathan, R., Ifju, P. G., & Quinn, R. D. A biologically inspired micro-vehicle capable of aerial and terrestrial locomotion. *Mechanism and Machine Theory*, 44(3):513 – 526, 2009. Special Issue on Bio-Inspired Mechanism Engineering.

- Bertram, J. E. & Gutmann, A. Motions of the running horse and cheetah revisited: fundamental mechanics of the transverse and rotary gallop. *Journal of The Royal Society Interface*, 35:549–559, 2009.
- Blanco, R. E. & Gambini, R. A biomechanical model for size, speed and anatomical variations of the energetic costs of running mammals. *Journal of Theoretical Biology*, 241(1):49 – 61, 2006.
- Blickhan, R. The spring-mass model for running and hopping. *Journal of Biomechanics*, 22(11-12):1217 – 1227, 1989.
- Chapman, R. F. *The insects: structure and function*. Cambridge University Press, 1998.
- Eich, M., Grimminger, F., Bosse, S., Spenneberg, D., & Kirchner, F. Asguard: A hybrid legged wheel security and sar-robot using bio-inspired locomotion for rough terrain. In *IARP/EURON Workshop on Robotics for Risky Interventions and Environmental Surveillance (IARP/EURON-08)*, 2008.
- Gasc, J.-P. Comparative aspects of gait, scaling and mechanics in mammals. *Comparative Biochemistry and Physiology - Part A: Molecular & Integrative Physiology*, 131(1):121 – 133, 2001.
- Hansen, N. & Ostermeier, A. Completely derandomized self-adaptation in evolution strategies. *Evolutionary Computation*, 9:159–195, 2001.
- Hansen, N., Muller, S., & Koumoutsakos, P. Reducing the time complexity of the derandomized evolution strategy with covariance matrix adaptation (CMA-ES). *Evolutionary Computation*, 11(1):1–18, 2003.
- Hoyt, D. & Taylor, C. Gait and the energetics of locomotion in horses. *Nature*, 292: 239–240, 1981.
- Ijspeert, A. J. Central pattern generators for locomotion control in animals and robots: A review. *Neural Networks*, 21(4):642 – 653, 2008. Robotics and Neuroscience.
- Kar, D. C., Issac, K. K., & Jayarajan, K. Gaits and energetics in terrestrial legged locomotion. *Mechanism and Machine Theory*, 38(4):355 – 366, 2003.
- Kern, S., Müller, S., Hansen, N., Büche, D., Ocenasek, J., & Koumoutsakos, P. Learning probability distributions in continuous evolutionary algorithms—a comparative review. *Natural Computing*, 3(1):77–112, 2004.

- Kirchner, F., Spenneberg, D., & Linnemann, R. *A biologically inspired approach towards robust real world locomotion in an 8-legged robot*. MIT-Press, Cambridge, MA, USA, 2002.
- Knight, R. & Nehmzow, U. Walking robots: a survey and a research proposal. Technical report, University of Essex, 2002.
- Kuehne, B. & Martz, P., editors. *OpenSceneGraph Reference Manual v2.2*. Skew Matrix Software, Blue Newt Software, 2007.
- Machowinski, J. *Dynamisches Laufen mit AsGuard*. Diploma Thesis, Dept. of Computer Science, University Bremen, 2009.
- Marey, J.-E. *Animal mechanism: a treatise on terrestrial and aerial locomotion*. Appleton and Co., 1874.
- McGeer, T. Passive dynamic walking. *Int. J. Robotics Research*, 9:68–82, 1990.
- McGhee, R. B. Some finite state aspects of legged locomotion. *Mathematical Biosciences*, 2(1-2):67 – 84, 1968.
- McMahon, T. A. & Cheng, G. C. The mechanics of running: How does stiffness couple with speed? *Journal of Biomechanics*, 23(Supplement 1):65 – 78, 1990.
- McMordie, D. & Buehler, M. Towards pronking with a hexapod robot. In *Int. Conf. Climbing and Walking Robots (CLAWAR)*, 2001.
- Morrey, J., Lambrecht, B., Horchler, A., Ritzmann, R., & Quinn, R. Highly mobile and robust small quadruped robots. In *Proceedings. 2003 IEEE/RSJ International Conference on Intelligent Robots and Systems*, 2003.
- Murphy, J. E., Carr, H., & O'Neill, M. Grammatical evolution for gait retargeting. In *In: Proc. Theory and Practice of Computer Graphics*, 2008.
- Muybridge, E. *Animals in motion*. Dover Publications, Inc., 1887.
- Neville, N., Buehler, M., & Sharf, I. A bipedal running robot with one actuator per leg. In *IEEE Int. Conf. Robotics and Automation (ICRA)*, 2006.
- Nieuwenhuys, R., Donkelaar, H. J., & Nicholson, C. *The central nervous system of vertebrates*. Springer, Berlin, 1997.
- Noor, K., Doyle, R., & Venneri, S. Autonomous, biologically inspired systems for future space missions. *Advances in Engineering Software*, 31:473–480, 2000.

- Olszta, M. J., Cheng, X., Jee, S. S., Kumar, R., Kim, Y.-Y., Kaufman, M. J., Douglas, E. P., & Gower, L. B. Bone structure and formation: A new perspective. *Materials Science and Engineering: R: Reports*, 58(3-5):77 – 116, 2007.
- Ostermeier, A., Gawelczyk, A., & Hansen, N. A derandomized approach to self-adaptation of evolution strategies. *Evolutionary Computation*, 2(4):369–380, 1994.
- Pfeifer, R., Lungarella, M., & Iida, F. Self-organization, embodiment, and biologically inspired robotics. *Science*, 318:1088–1093, 2007.
- Quinn, R., Nelson, G. M., Bachmann, R. J., & Ritzmann, R. E. Toward mission capable legged robots through biological inspiration. *Autonomous Robots*, 11: 215–220, 2001.
- Quinn, R., Kingsley, D., Offi, J., & Ritzmann, R. Improved mobility through abstracted biological principles (2002). In *IEEE Int. Conf. On Intelligent Robots and Systems (IROS'02)*, 2002.
- Rayner, J. M. Gravity, the atmosphere and the evolution of animal locomotion. In Rothschild, L. J. & Lister, A. M., editors, *Evolution on Planet Earth*, pages 161 – 183. Academic Press, London, 2003.
- Rechenberg, I. Case studies in evolutionary experimentation and computation. *Computer Methods in Applied Mechanics and Engineering*, 186(2-4):125 – 140, 2000.
- Ritzmann, R. E., Quinn, R. D., & Fischer, M. S. Convergent evolution and locomotion through complex terrain by insects, vertebrates and robots. *Arthropod Structure & Development*, 33(3):361 – 379, 2004. Arthropod Locomotion Systems: from Biological Materials and Systems to Robotics.
- Ruina, A., Bertram, J. E., & Srinivasan, M. A collisional model of the energetic cost of support work qualitatively explains leg sequencing in walking and galloping, pseudo-elastic leg behavior in running and the walk-to-run transition. *Journal of Theoretical Biology*, 237(2):170 – 192, 2005.
- Römmermann, M., Edgington, M., Metzen, J. H., Fernandez, J. d. G., Kassahun, Y., & Kirchner, F. Learning walking patterns for kinematically complex robots using evolution strategies. In *10th International Conference on Parallel Problem Solving from Nature (PPSN-2008)*, 2008.

Saranli, U. & Buehler, M. Design, modeling and preliminary control of a compliant hexapod robot. In *Proceedings of the IEEE International Conference on Robotics and Automation (ICRA2000)*, 2000.

Saranli, U., Buehler, M., & Koditschek, D. Rhex: A simple and highly mobile hexapod robot. *Int. J. Robotics Research*, 20:616–631, 2001.

Scarfogliero, U., Stefanini, C., & Dario, P. The use of compliant joints and elastic energy storage in bio-inspired legged robots. *Mechanism and Machine Theory*, 44: 580–590, 2009.

Smith, C. U. *Biology of sensory systems. 2nd ed.* Chichester: Wiley-Blackwell., 2009.

Thakoor, S. Bio-inspired engineering of exploration systems. *J. Space Mission Architecture*, 2:49–79, 2000.

Todd, D. *Walking machines - An introduction to legged robots.* Chapman and Hall, 1985.

Vaughan, C. L. & O’Malley, M. J. Froude and the contribution of naval architecture to our understanding of bipedal locomotion. *Gait & Posture*, 21(3):350 – 362, 2005.

Vincent, J. F. & Wegst, U. G. Design and mechanical properties of insect cuticle. *Arthropod Structure & Development*, 33(3):187 – 199, 2004. Arthropod Locomotion Systems: from Biological Materials and Systems to Robotics.

Webb, B. Using robots to model animals: a cricket test. *Robotics and Autonomous Systems*, 16:117–134, 1995.

Weingarten, J., Lopes, G., Grodd, R. E., Buehler, M., & Koditschek, D. Automated gait adaptation for legged robots. In *IEEE Int. Conf. Robotics and Automation (ICRA)*, 2004.

List of Figures

1.1	Hybrid Walking Robots. RHex: Kod*lab, University of Pennsylvania (http://kodlab.seas.upenn.edu); Whegs: Center for Biologically Inspired Robotics Research, Case Western University (http://biorobots.cwru.edu/projects/whegs/); AsGuard: Deutsches Forschungszentrum für Künstliche Intelligenz (DFKI)	4
1.2	Diagrams of a number of quadruped gaits with relative phases of leg movements and common names (Alexander, 1984).	6
1.3	A gait diagram with duty factors illustrated as length of the bars, taken from Kar et al. (2003).	7
1.4	Transitions from symmetrical to asymmetrical gaits of various quadrupeds such as dogs (●), ferrets (○) and rats (□) between Fr=2 and Fr=3, taken from Alexander and Jayes (1983).	8
1.5	Stance phases and parameters of star wheels.	10
1.6	AsGuard V2. Source: DFKI	12
2.1	The physical model of the robot in MARS.	16
2.2	Scheme of the controller used in the experiments.	19
3.1	Typical development of fitness function values over generations in the optimisation for speed (N=7).	25
3.2	Typical development of fitness function values over generations in the optimisation for vertical displacement with Fr=0.56 (N=3, mode _c).	26
3.3	Average fitness values achieved for each of the eight scenarios over average Froude number, both for continuous and non-continuous driving of the wheels.	27
3.4	Evolved relative phases for optimisation of vertical displacement.	29
3.5	Relative phases of selected evolved gaits (illustration inspired by Alexander 1984). Values of Φ_{HL} and Φ_{HR} are chosen arbitrarily where applicable.	30
3.6	Gait diagrams for two of the gaits observable at higher speeds.	30

3.7	Mean vertical deviation of the COM from its average vertical position for selected gaits over varying Froude numbers for both $mode_c$ (left) and $mode_n$ (right).	31
3.8	Height over ground of COM over time for continuous (a, b) and non-continuous driving (c, d) with different gaits.	32
3.9	Angles of Attack over speed	33

List of Tables

1.1	Angle between legs γ and maximum angle of attack α_{max} for different values of n_l (number of legs) of a star wheel.	11
2.1	Fixed values of the four motor controller parameters during vertical displacement optimisation.	23
2.2	Froude numbers, turning frequencies and rotational velocities for the evolution runs optimising for vertical deviation	24
3.1	Combined results of both runs and all scenarios of the vertical displacement minimisation evolutions.	28

DECLARATION OF AUTHORSHIP

I, Kai Alexander von Szadkowski, declare that this thesis and the work presented in it are my own and has been generated by me as the result of my own original research "Evolution of Gaits in a Simulated Hybrid Leg-Wheel Robot"

I confirm that:

1. Where any part of this thesis has previously been submitted for a degree or any other qualification at this University or any other institution, this has been clearly stated;
2. Where I have consulted the published work of others, this is always clearly attributed;
3. Where I have used graphics I did not create myself, the source is given;
4. Where I have quoted from the work of others, the source is always given. With the exception of such quotations, this thesis is entirely my own work;
5. Where the thesis is based on work done by myself jointly with others, I have made clear exactly what was done by others and what I have contributed myself;
6. None of this work has been published before submission.

Date:

Signed: